# Microstructure and interfaces in diamond coated steel wires

P. G. PARTRIDGE, C. M. YOUNES, J. NICHOLSON, G. MEADEN, E. D. NICHOLSON*
*Interface Analysis Centre and *School of Chemistry, University of Bristol, Bristol, UK*
S. BLEAY, C. GILMORE
*Structural Materials Centre DRA (Farnborough) Hants, GU14 OLX*

Diamond fibres were produced in a hot filament reactor by chemical vapour deposition of a 40 μm thick layer of diamond on to titanium-coated iron and iron–chromium wires. In the 40 h deposition time carbon diffused through the titanium and steel and produced carbide microstructures with hardness values of ~3234 and 5390 N mm$^{-2}$ for the Fe and Fe–Cr cores, respectively. During cooling thermal stress fracture of the diamond was avoided by stress relief cracks in the disordered graphite layer at the diamond/Ti-rich layer interface.

## 1. Introduction

Diamond offers an attractive combination of physical, mechanical and chemical properties [1]. Thin diamond coatings produced by chemical vapour deposition (CVD) have properties almost identical to those of natural diamond [2]. Such coatings may be used for their wear resistance, grinding or machining ability, thermal conductivity and corrosion resistance. Recently diamond fibres have been manufactured by CVD on to thin metallic wire or ceramic cores [2, 3, 4]. These fibres may enable the very high elastic modulus of diamond to be exploited in fibre-reinforced composites [3, 4, 5].

The properties of a diamond fibre can be modified by selecting a suitable core material. However, there are four major requirements for the core material: a surface that encourages diamond nucleation; adequate chemical stability in the activated hydrogen/methane gas mixtures used in the diamond deposition process; adequate mechanical strength to withstand a deposition temperature of 900–1000 °C; and thermal expansion compatibility with diamond. A SiC fibre or a tungsten wire satisfies these requirements, with the latter initially forming a thin stable tungsten carbide interface layer [6]. Diamond deposition is more difficult on metallic substrates that form solid solutions with carbon such as iron [7, 8, 9], nickel [10, 11, 12] and titanium [13, 14]. Deposition of diamond on to ferrous materials is of particular interest, because of their low cost and widespread use. Furthermore, a ferrous wire core would be an attractive low cost, low density alternative to tungsten wire cores for diamond fibres. However, diamond films deposited directly on steels exhibit poor adhesion and high residual stresses, which leads to delamination of the diamond coating. To avoid this problem, a number of interlayers have been considered [7, 8, 9]. In order to assess the potential of steel wires for fibre cores, diamond deposition has been carried out on titanium coated iron and iron–chromium wires. The microstructure and interfaces in the diamond coated wires are described in this paper and compared with data reported for diamond deposits on flat substrates.

## 2. Experimental technique

Iron and iron–chromium steel wires were used with nominal compositions (wt %) of Fe 99.5 and Fe–13Cr–4.8Al–0.3Si–0.3Y, respectively. The wires were about 200 mm long and 0.05 or 0.125 mm diameter. A titanium layer about 5–7 μm thick was magnetron sputter coated on to the wires prior to diamond deposition in a Thomas Swan CVD hot filament reactor [2]. The deposition conditions were methane/hydrogen gas mixture ratio 1:100, gas flow rate of 200 s.c.c.m. at $39.99 \times 10^2$ Pa pressure, a filament temperature of ~2000 °C, a radiantly heated fibre temperature of ~900 °C, giving a mean diamond deposition rate of ~1 μm h$^{-1}$. The deposition time was ~40 h. The coated fibres were cooled rapidly to about 350 °C when the hot filament was switched off. Fibres were cut with a scalpel or an excimer laser. Microhardness values for the fibre core were determined with a pyramidal diamond indenter under a 200 g load on a diamond polished longitudinal cross-section. Chemical analysis of the CVD diamond/Ti and Ti/steel wire interfaces was performed using scanning Auger microscopy (SAM). The analysis was made on fibre fracture surfaces produced by cantilever bending within the ultra-high vacuum of a Perkin-Elmer PHI 595 SAM system. This avoided contamination of the interfaces by C, O and N that occurs when fractures are made in air and which precludes accurate measurement of these elements.

0022–2461  

## 3. Results

After careful fracture of the fibre in bend, it was found that the fibre core had deformed and one or more cracks were visible at the diamond/Ti layer or to a lesser extent at the Ti layer/steel wire interfaces. Ablation of the core material during laser cutting obscured the interfaces. A fractured diamond fibre with a 50 μm diameter Fe-wire core and ~40 μm thick diamond coating is shown in Fig. 1a. The cross-section revealed the characteristic columnar grains of the outer diamond coating. The grains were oriented with their long axes parallel to the radial directions and surface facets were produced where the grains intersected the fibre surface. The grain diameters at the surface were less than 10 μm. The thin Ti-rich layer appeared to have deformed away from the diamond coating and the transverse fracture surface of the core was rough (Fig. 1b). The volume fraction of diamond in the fibre was about 80%.

Wires with a larger diameter of 125 μm were used in order to make measurements on the fibre core easier. A similar transverse fracture of a fibre with a 125 μm diameter Fe–Cr wire core and ~36 μm thick diamond deposit is shown in Fig. 2. Similar deformation of the Ti layer was observed, but the core cross-section was less rough than for the Fe-wire core. The diamond volume fraction was about 60%. A characteristic CVD diamond Raman spectrum obtained using a He–Ne laser on the fibre surface (Fig. 3) showed a peak at wave number 1333 $cm^{-1}$, corresponding to $sp^3$ diamond, and a broad peak at 1580 $cm^{-1}$ corresponding to $sp^2$ graphite.

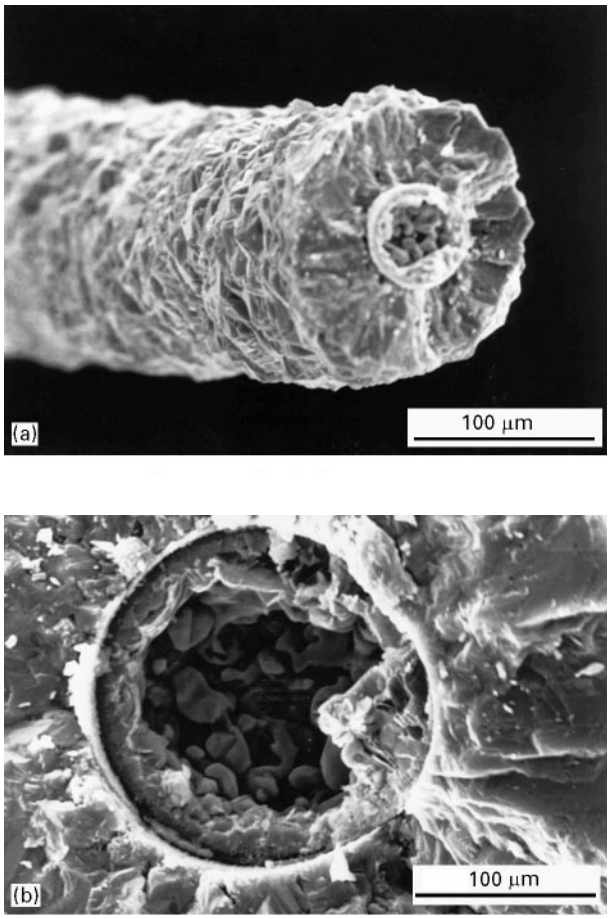


*Figure 1* Diamond fibre. (a) Transverse fracture of diamond coating on Ti-coated 50 μm diameter Fe wire. (b) Detail of core fracture showing deformation in Ti-rich layer and rough fracture of Fe-rich core.

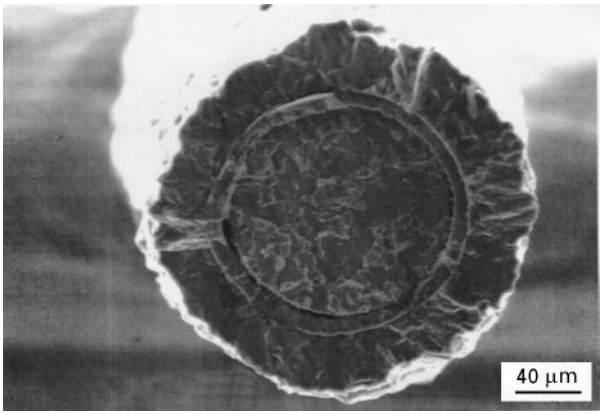


*Figure 2* Transverse fracture of diamond coating on Ti-coated 125 μm diameter Fe–13%Cr wire core.

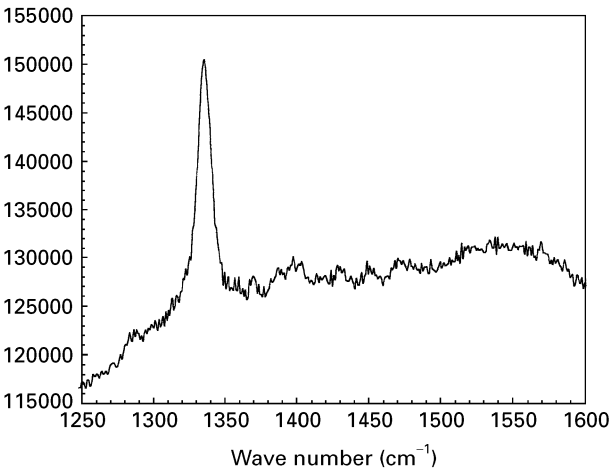


*Figure 3* Raman spectrum from surface of fibre, showing diamond peak at 1333 $cm^{-1}$ and broad graphite peak at 1580 $cm^{-1}$.

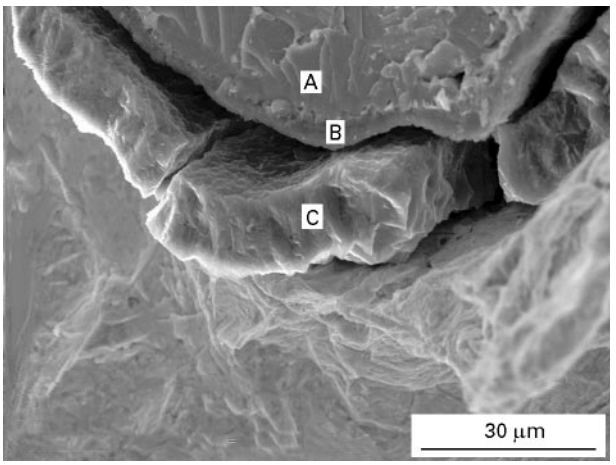


*Figure 4* Coated Fe–13%Cr wire fractured in the UHV of the Auger spectrometer. Fe-rich core at A, Ti-rich coating at B, diamond coating at C.

### 3.1. Auger spectroscopic analysis

SAM analysis using the spot mode was carried out on fibre cross-sections produced by fracture under a background pressure of $< 1.333 \times 10^{-7}$ Pa. The transverse fracture of the Fe–Cr core fibre (Fig. 4) showed the cracked diamond coating at C and the thin Ti-rich layer at B which remained attached to the steel core at A and exposed the diamond/Ti layer interface. No Ti or other metals were detected on the inner fractured surface of the diamond. Diamond nucleation has been reported to be associated with a thin amorphous carbon (α-carbon) or disordered graphite layer on Fe [8], Ni [12] and Ti [14] substrates. It was concluded that the fracture plane in the fibre core lay in this disordered graphite.

The layers on a fibre before and after diamond coating are shown schematically in Fig. 5a–c. The relative atomic concentration of C, Fe, and Ti in the Fe cored fibre are plotted versus distance from the outer surface of the Ti layer in Fig. 6a. The results indicate that during diamond deposition at $\sim 900\,^{\circ}C$, all the interfaces were in contact (Fig. 5b) and carbon

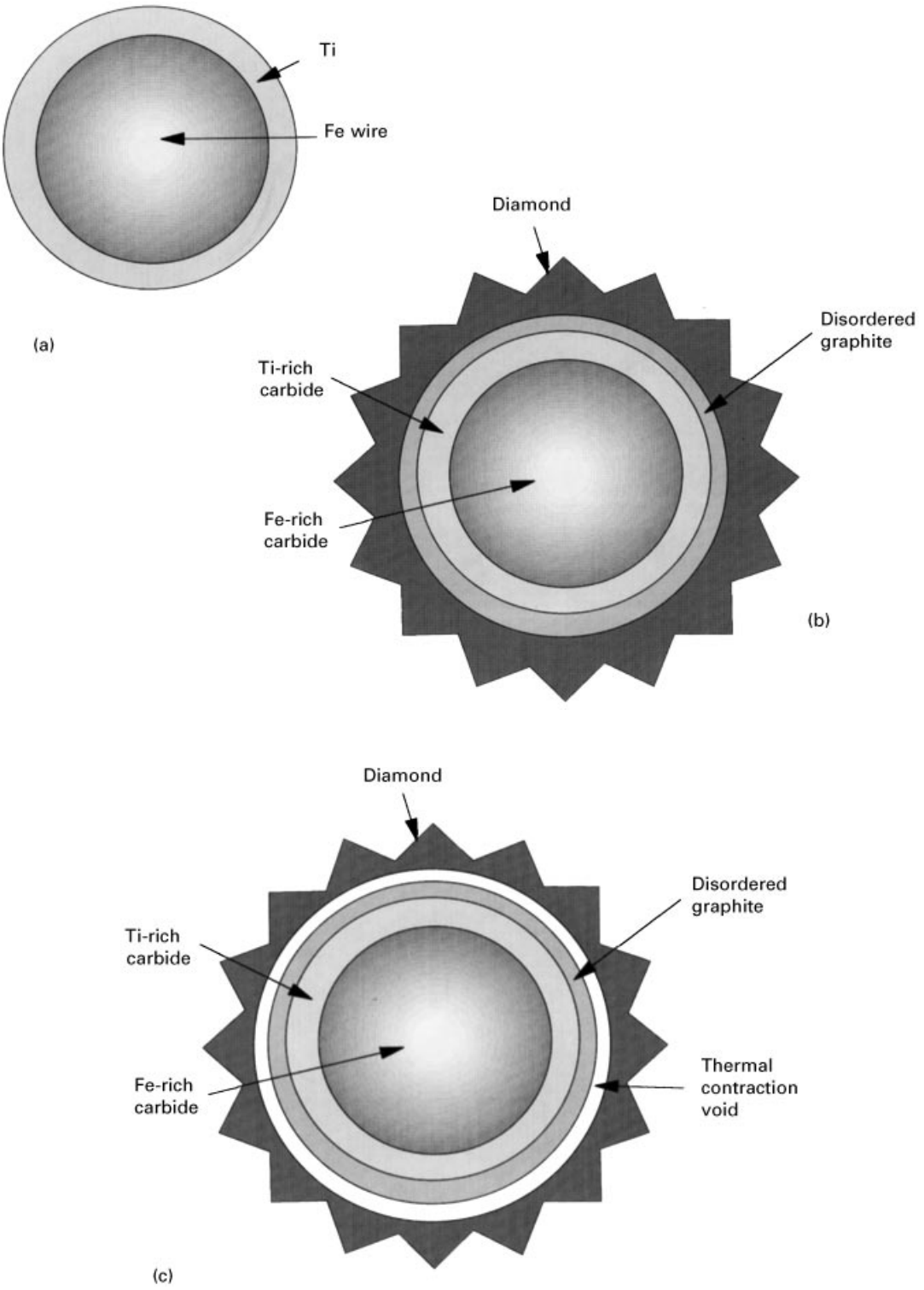


*Figure 5* Schematic of coated wire. (a) Ti sputter-coated wire at ambient temperature; (b) at 900 °C after diamond coating; (c) after cooling to ambient temperature, showing void produced by thermal contraction of core.

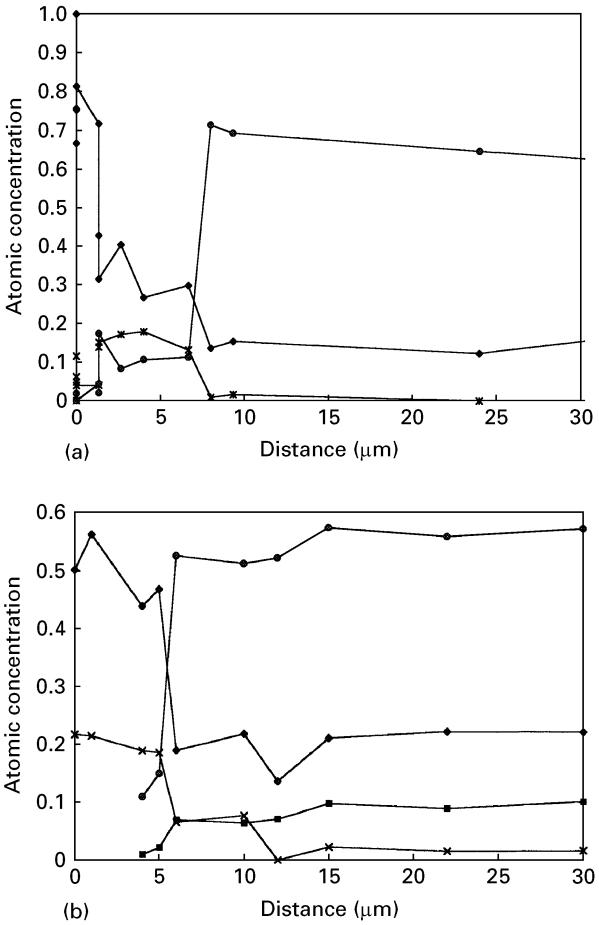


*Figure 6* Concentration of C, Ti, Cr and Fe versus distance from outer surface of Ti-rich layer into the Fe-rich core as measured by SAM. (a) Fe wire core. (b) Fe–Cr wire core. (⊗) Fe; (◆) C; (■) Cr; (×) Ti.

diffused through the thick Ti-rich layer into the wire core and Fe diffused into the Ti layer from the steel. The high concentration of carbon ( ~10 at %, 2.3 wt %) indicates both the Ti layer and the steel core were carburized. Oxygen was also detected in the Ti-rich layer as shown in the Auger spectrum for the Fe–Cr fibre in Fig. 7. The presence of oxycarbides was indicated by the shape of the C peak and the shortening of the high energy Ti peak in the presence of oxygen. Oxygen has been reported for CVD diamond coatings on Ti substrates and attributed to the initial surface oxides on the Ti surface [14]. Thus the formation of stable Ti oxycarbides is possible in the Ti-rich region. The corresponding concentration versus distance curves are shown for the Fe–Cr cored fibre in Fig. 6b. A higher concentration of carbon ( ~ 20 at %, 5.1 wt %) in the Fe–Cr core was found than in the corresponding Fe core. This result is consistent with the Fe and Cr elements in the steel core being largely converted to the corresponding carbides. These high carbon concentrations are typical of hyper-eutectoid steels and white cast irons [15]. In the Fe alloy fracture, one analysis indicated a composition of 100% carbon. This may have been caused by some precipitation of grain boundary graphite.

## 3.2. Microstructure

It was impossible to polish a planar cross-section of a diamond fibre, because the harder diamond coating always protruded above the surrounding material and prevented the polishing of the core. The diamond coating was therefore deliberately fractured and removed leaving most of the Ti rich layer on the steel core. Longitudinal polished sections of the core were then obtained and etched in dilute nitric acid. The core microstructures were produced initially under isothermal conditions at the diamond deposition temperature of ~ 900 °C for about 40 h before cooling rapidly to 350 °C, when the filament was switched off.

Taking the Fe-core composition of 2.3 wt % C in the Fe–$Fe_3C$ phase diagram in Fig. 8 [17], the optical micrograph in Fig. 9a–b was consistent with primary

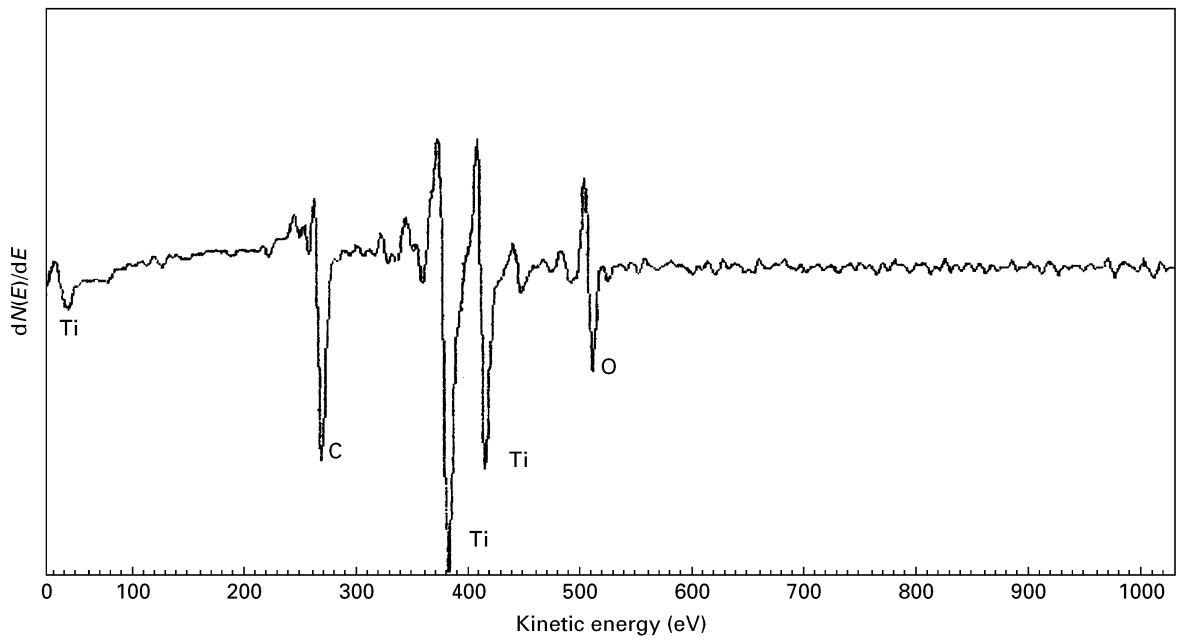


*Figure 7* A differentiated Auger electron spectrum recorded from the titanium oxycarbide layer between the CVD diamond film and the Fe–Cr core.

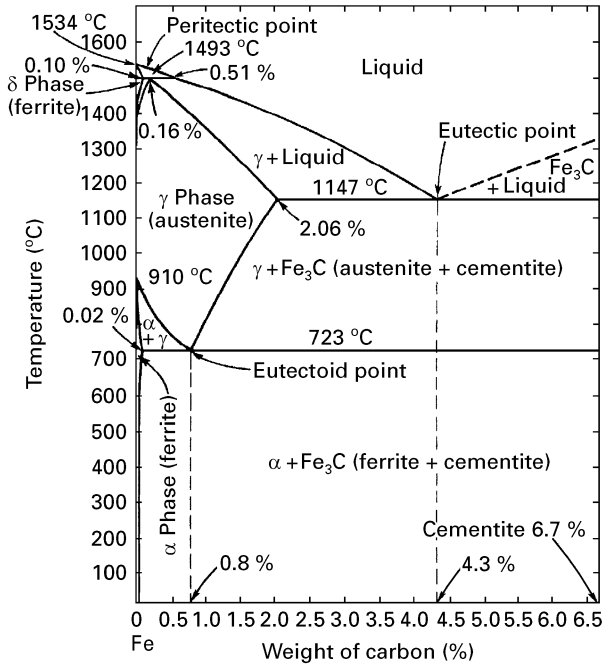


*Figure 8* Fe–$Fe_3C$ phase diagram (after ref. 16).

$Fe_3C$ (light coloured non-etching areas) in dark etching lamellar eutectoid pearlite containing small unetched hypereutectoid $Fe_3C$ grains. The thin Ti-rich layers are visible at the edge of the section in Fig. 9a. The Ti-rich layer was discontinuous in places at X and Y. Here there was evidence of surface reactions producing a different phase.

The sections through the 5.1 wt % C composition Fe–Cr core (Fig. 10a) showed larger areas of unetched $Fe_3C$ and a distribution of dark and lighter etching phases, believed to be eutectoid pearlite and Cr carbide. No lamellar structures were visible. The 5 μm thick Ti-rich layer (Fig. 10b) appeared continuous but etched in places at its inner interface. No surface reaction sites were found. It is clear that diamond/core fracture had occurred at the outer surface of the Ti-rich layer.

An as received Fe–Cr wire control specimen and a diamond coated Fe–Cr wire were immersed in concentrated hydrochloric acid for 4 days. After this treatment the control sample had completely dissolved. The diamond on the coated wire was unaffected (Fig. 11a–b) and the core and Ti layer remained but were pitted, with the outermost Ti region appearing particularly resistant to etching, as in Fig. 10b. The unetched $Fe_3C$ phase in Fig. 10a remained as a network in the core at A in Fig. 11b. A view of an etched region where the diamond coating had been partly fractured (Fig. 12a) showed two distinct layers, B and C, between the core at A and the unetched diamond. Energy-dispersive analysis of X-ray (EDAX) images for Fe and Cr in Fig. 12b–c and for Ti in Fig. 12d confirmed the A surface corresponded to the steel core and the B surface to the Ti-rich layer. Since no significant amount of metallic material was detected in the C layer next to the inner diamond surface, this was believed to be the disordered graphite layer in which fracture occurred.

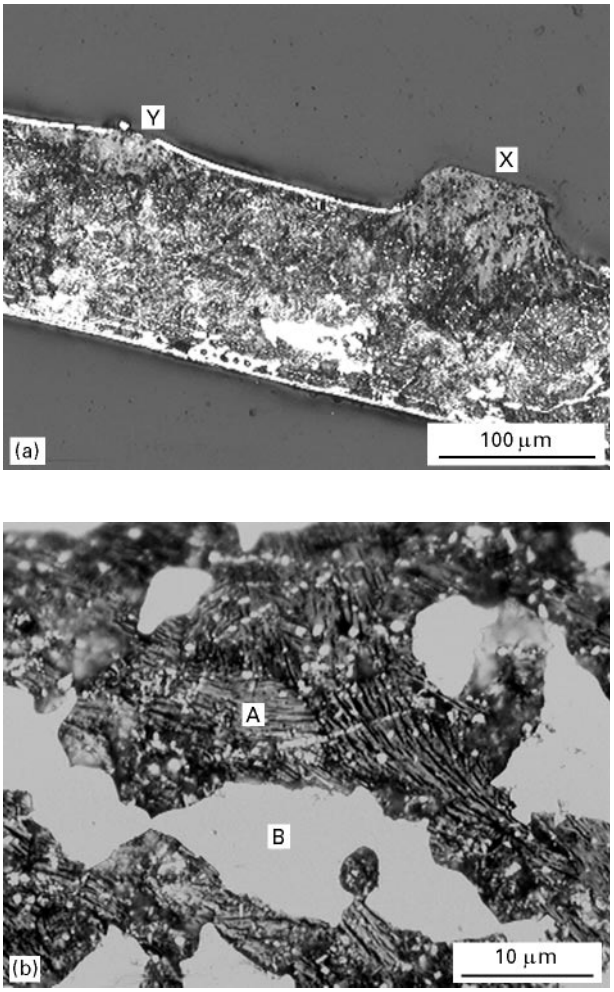


*Figure 9* Optical micrographs of polished and etched longitudinal sections of Fe wire fibre cores after diamond removed: (a) dark areas pearlite type microstructure, light areas $Fe_3C$, Ti-rich layer at edge of section, with breaks at X and Y associated with interface reactions; (b) pearlite type microstructure at A, and $Fe_3C$ at B.

### 3.3. Hardness

Microhardness values obtained for longitudinal polished sections of the fibre cores before and after diamond coating are given in Table I. Large increases in hardness were obtained after diamond coating, with values of 3234 and 5390 $N\,mm^{-2}$ for the iron and Fe–Cr alloy cores respectively, in agreement with the amount of carbide observed. The measured core carbon contents and microstructures are characteristic of tool steel and white cast iron [15]. The reported hardness values for these materials of 3332 and 4704–6272 $N\,mm^{-2}$ (Table I), are in agreement with the measured core hardness values. An additional contribution to the hardness of the Fe–Cr core is expected from chromium carbide formation. There are several carbides, with $Cr_3C_2$ having a hardness of 13.98 $kN\,mm^{-2}$. The Ti-rich layer is also expected to have a high hardness based on TiC, with a value of 28.86 $kN\,mm^{-2}$ (Table I).

## 4. Discussion

The results show that Ti-coated steel wires can be used to produce diamond fibres. Diamond nucleated on the sputter-coated titanium but titanium did not provide

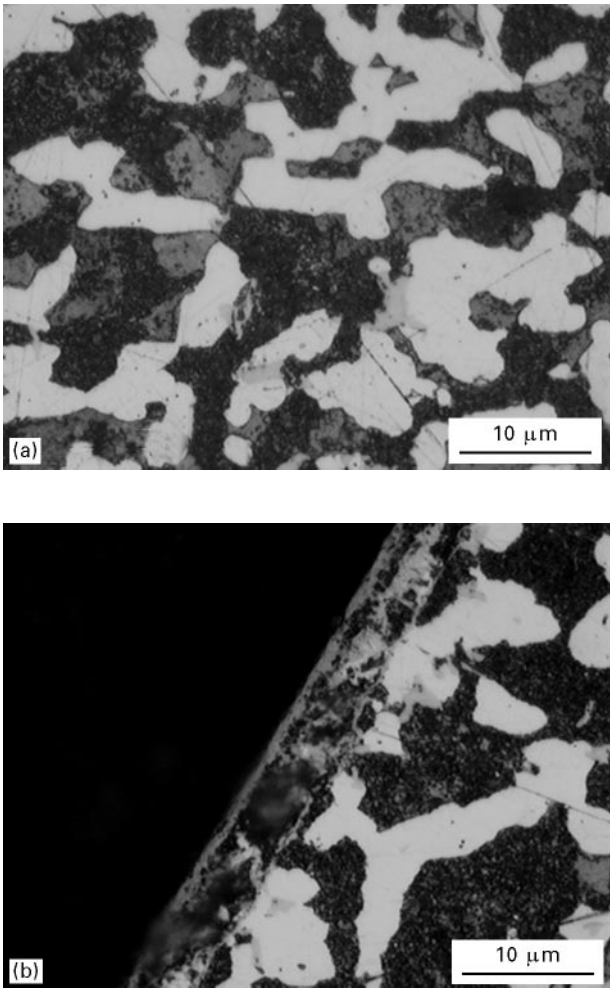


*Figure 10* Optical micrographs of polished and etched longitudinal sections of Fe–Cr wire fibre cores after diamond removed: (a) dark areas pearlite and Cr carbides, light areas $Fe_3C$; (b) continuous Ti-rich interface layer.

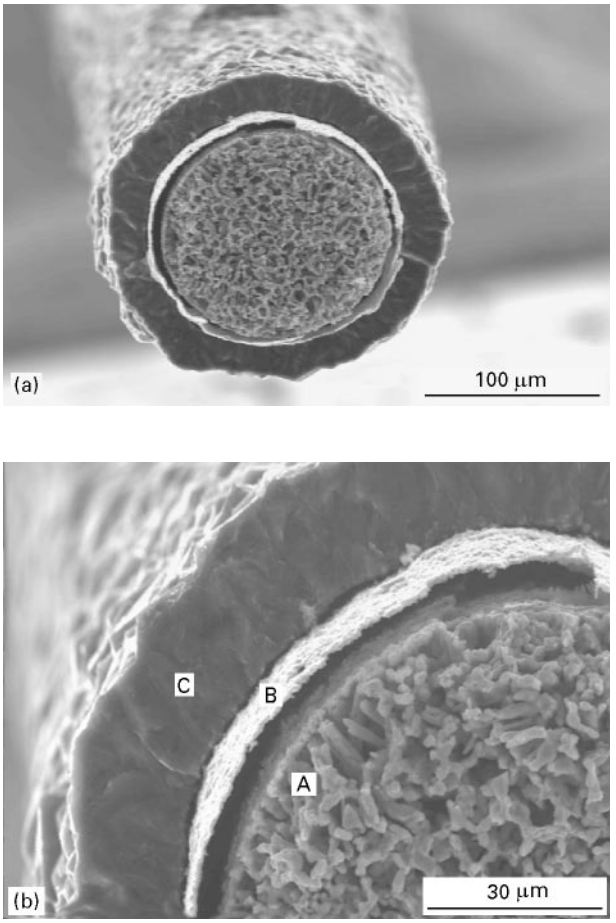


*Figure 11* Transverse fracture Fe–Cr wire fibre after chemical etching for 4 days in concentrated HCl: (a) fibre cross-section; (b) carbide network in Fe-rich core at A, Ti-rich layer at B, diamond at C.

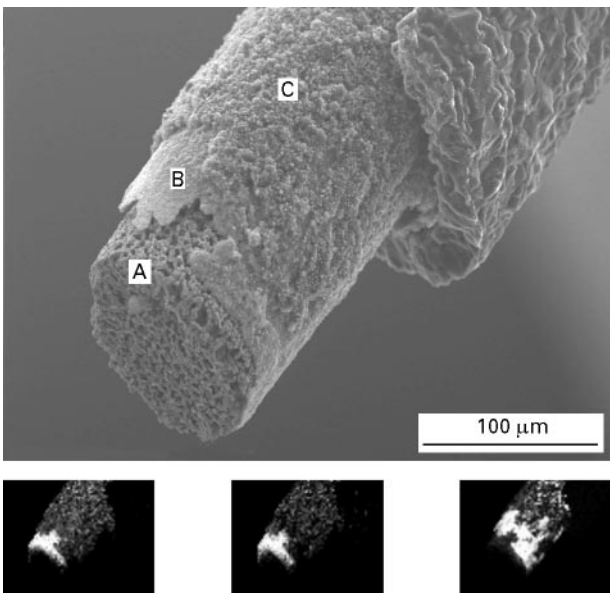


*Figure 12* Longitudinal surface of Fe–Cr wire fibre after etching for 4 days in concentrated HCl: (a) Fe-rich core at A, Ti-rich layer at B, disordered graphite at C, with diamond outer layer. EDAX image for (b) Fe, (c) Cr (d) Ti.

a barrier to carbon diffusion. It is difficult to measure accurately the temperature of the radiantly heated wires in the reactor and it is possible for the Ti to be in the β-phase. Diffusion rates would be orders of magnitude greater than for the α-phase, and may allow rapid carburization of the core before forming TiC. Diamond deposition required long times at about 900 °C, and diffusion of C into the iron core under isothermal conditions would have produced $Fe_3C$ and chromium carbides in the presence of Cr. On cooling there was evidence of precipitation of $Fe_3C$ in the peritectic form, but the composition, microstructure and hardness data suggest the cores consist largely of carbide phase after diamond coating. The $Fe_3C$, unlike other transition metal carbides, is metastable at low temperatures and can form graphite. The Auger analysis indicated some grain boundary graphite may have formed in the Fe core.

The sections showed the Ti-rich coating was continuous beneath the diamond deposit on the Fe–Cr core. This is an important result, since it indicates that during heating to the diamond deposition temperature, when the steel expanded more than the Ti (Table I), the Ti sputter coating plastically deformed without cracking. Similar experiments using a W coating led to multiple cracks in the W because of the greater thermal expansion mismatch (Table I) and lower ductility of the W. Some breaks were found in the Ti-rich coating on the Fe core. Since the expansion mismatch was about the same for Fe and Fe–Cr,

TABLE I Hardness, density and thermal expansion values [15, 17, 18]

| Material composition (wt %) | Diamond pyramid hardness $N\,mm^{-2}$ | Density $mg/m^3$ | Thermal expansion $10^{-6}\,K^{-1}$ |
|---|---|---|---|
| 99.5 Fe-wire | 588–686 | 7.87 | 12.1 |
| Diamond coated | core | | |
| 99.5 Fe core | 3165–3292 | | |
| Fe–13Cr–4.8Al–0.3Si–0.3Y wire | 1832.6 | 7.22 | 11.1 |
| Diamond coated | core | | |
| Fe–13Cr–4.8Al–0.3Si–0.3Y wire | 4851–5762.4 | | |
| Normalized tool steel (high carbon, 1.2–1.5 C) | 3332 | | |
| White cast iron (high carbon, 3.25 C, 0.25 Si) | 4704–6272 | | 11.9 |
| W-wire | 3528 | 19.3 | 4.5 |
| Ti | 588 | 4.5 | 8.9 |
| TiC | $28.86 \times 10^3$ | 4.93 | 7.7 |
| $Fe_3C$ | 7840–9800 | 7.69 | |
| $(FeCr)_3C$ | 8134–13426 | | |
| $(FeCr)_7C_3$ | $12.02–14.45 \times 10^3$ | | |
| Cr | 2156 | 7.1 | 4.9 |
| $Cr_3C_2$ | $13.98 \times 10^3$ | 6.68 | 10.3 |
| CVD diamond | $30.96–89.90 \times 10^3$ | 3.5 | 0.8–1.0 |

chromium appeared to be responsible for the absence of cracks in the Ti-rich coating on the Fe–Cr core. Chromium combined with nitrogen has been reported to be an effective barrier to carbon diffusion [8]. With the higher hardness of the (FeCr) carbides (Table I), a greater depth of hardening may be obtained compared with Fe carbide alone, reducing the tendency for the Ti(O)C layer to crack.

Since CVD diamond has a very small thermal expansion coefficient ( $\sim 1 \times 10^{-6}\,°C^{-1}$), high thermal mismatch stresses of $\sim 7$ GPa can arise in diamond coatings on titanium alloy [12] and ferrous materials [8, 9] (thermal expansion coefficients of $8.9 \times 10^{-6}\,°C^{-1}$ and $11–12 \times 10^{-6}\,°C^{-1}$ respectively (Table I)). However, 200 mm long straight diamond-coated wires were obtained in the present experiments with no apparent cracking, although the thermal expansion coefficients of carbides are close to the values for Ti and steel (Table I). There was evidence of considerable plasma mixing of carbon, oxygen and Ti species in a Ti-rich layer between CVD diamond and a Ti substrate [13], and this region is expected to be very hard. The thermal mismatch stresses appear to be relieved therefore by cracks in the less hard thin graphitic carbon layer C at the interface between the diamond and the Ti-rich B layer, as shown in Fig. 12 and schematically in Fig. 5c. This "fail-safe" weak interface allowed the steel core to contract away from the diamond during cooling. In this system the graphite layer may fulfil an important role in allowing axially symmetric shapes with high thermal expansion to be coated with diamond while avoiding cracks and residual stresses in the diamond and reducing sensitivity to thermal cycles. However, it should be noted that kinks or bends in the wire can give rise to thermal cracking in the diamond deposit.

The stress relief cracking in the C layer leads effectively to a hollow diamond fibre with a loose core. This can have other advantages for fibres in a composite. For example, with large $t/D$ ratios, where $t$ = diamond film thickness, $D$ = core diameter, the fibre strength and stiffness will be dictated by the diamond volume fraction. Assuming the core does not transmit any load, a core with a high thermal expansion coefficient may be made *in situ* with selected physical properties, without regard to its mechanical properties or thermal mismatch. Thus fibres with magnetic or resistive heating properties may be obtained [19].

## 5. Conclusions

Titanium coated iron and iron–chromium wires can be coated with diamond by chemical vapour deposition, but after depositing for 40 h the fibre cores were converted to very hard carbide microstructures. During the cooling of straight diamond coated wires, thermal stress cracking of the diamond was avoided by stress relief cracking in the disordered graphite layer at the diamond/Ti-rich layer interface. This effectively leads to a hollow diamond fibre with a loose core, and with the fibre strength and stiffness determined by the diamond volume fraction only. This allows a core to be formed *in situ* with selected physical properties, without regard to its mechanical properties or thermal mismatch.

## Acknowledgements

The authors wish to thank Professors Ashfold (Chemistry), Steeds (Physics) and Allen (Interface Analysis Centre) and N. Everitt for providing facilities and EPSRC and DRA (Farnborough) for financial support.

## References


1. J. E. FIELD, "Properties of diamond". (Academic Press, London, 1979).
2. P. G. PARTRIDGE, P. W. MAY and M. N. R. ASHFOLD, *Mater. Sci. Technol.* **10** (1994) 177.
3. P. G. PARTRIDGE, P. W. MAY, C. A. REGO and M. N. R. ASHFOLD, *ibid.* **10** (1994) 505.
4. M. N. R. ASHFOLD, P. W. MAY, E. D. NICHOLSON, P. G. PARTRIDGE, G. MEADEN, A. WISBEY and M. J. WOOD, in Proceedings of Applications of Diamond Films and related Materials. Third International Conference, 1995, edited by A. Feldman, Y. Tzeng, W. A. Yarbrough, M. Yoshikawa and M. Murakawa, (National Institute of Standards and Technology, Gaithersburg, USA, 1995) p. 529.
5. E. D. NICHOLSON, J. E. FIELD, P. G. PARTRIDGE and M. N. R. ASHFOLD, *Mater. Res. Soc.* **283** (1996) 101.
6. Q. S. CHIA, C. M. YOUNES, P. G. PARTRIDGE, G. C. ALLEN, P. W. MAY and C. A. REGO, *J. Mater. Sci.* **29** (1994) 6397.
7. M. NESLADEK, C. ASINARI, J. SPINNEWYN, R. LEBOUT, R. LORENT and M. D'OLIESLAEGER, *Diamond and Related Materials*, **3** (1994) 912.
8. A. FAYER, O. GLOZMAN and A. HOFFMAN, *Appl. Phys. Lett.* **67** (1995) 2299.
9. M. D. DRORY, in Proceedings of Applications of Diamond Films and Related Materials Third International Conference, edited by A. Feldman, Y. Tzeng, W. A. Yarbrough, M. Yoshikawa, M. Murakawa (National Institute of Standards and Technology, Gaithersburg, USA, 1995) p. 313.
10. V. P. GODBOLE and J. NARAYAN, *J. Mater. Res.* **7** (1992) 2785.
11. X. QIAO, O. FUKUNAGA, T. TSURUMI, N. OHASHI, N. SHINODA and K. YUI, "Advances in new diamond science and technology" (M Y U, Tokyo, 1994) p. 195.
12. Y. SATO, H. FUJITA, T. ANDO, T. TANAKA and M. KAMO, *Phil. Trans. R. Soc.* **A342** (1993) 225.
13. J. W. AGAR, M. D. DRORY, *Phys. Rev.* **B48** (1993) 2601.
14. S. S. PERRY, J. W. AGER, G. A. SOMORJAI, R. J. McCLELLAND and M. D. DRORY, *J. Appl. Phys.* **74** (1993) 7542.
15. O. H. WYATT and D. DEW-HUGHES, "Metals, ceramics and polymers" (Cambridge University Press, Cambridge, 1974) pp. 156, 484.
16. M. HANSEN and K. ANDERKO, "Constitution of binary alloys" (McGraw-Hill, 1958) p. 353.
17. H. T. ANGUS, "Cast iron: physical and engineering properties" (Butterworths).
18. P. ETTMAYER and W. LENGAUER, "Encyclopedia of inorganic chemistry" (J. Wiley, Chichester, 1994) p. 519.
19. P. G. PARTRIDGE *et al.* Unpublished work.



*Received 8 June*
*and accepted 3 September 1996*